2025 International Conference on Intelligent Computing
July 26-29, Ningbo, China
https://www.ic-icc.cn/2025/index.php

A New Method of Exploring the Parameters of Heston Option Pricing Model: Multi-Population Genetic Algorithm

Yan Fang[1][0000-0002-9780-7956], Chang Guan[1] and Julius Wu[2]

[1] Shanghai University of International Business and Economics, Shanghai, 201620, China
[2] University of California, Davis, CA, United States, 95616
yiffanyfang163.com

Abstract. Accurate option pricing remains a key challenge in financial markets. The Heston model, a widely adopted stochastic volatility framework, improves pricing performance by accounting for time-varying volatility. However, its effectiveness critically depends on the accurate calibration of model parameters. To address the limitations of traditional calibration methods, this study introduces a novel framework that applies a multi-population genetic algorithm to search for the optimal parameter values for the Heston model. The calibrated parameters are then used to generate model-implied option prices. The framework is empirically evaluated using option data from both the SSE 50ETF and the Hang Seng Index. The results show that the proposed method provides more accurate parameter estimates, and outperforms conventional approaches in both pricing accuracy and computational stability. Moreover, it exhibits consistent performance across both developed and emerging markets, underscoring its practical value for financial derivative valuation.

Keywords: Heston Model, Multi-Population Genetic Algorithm, Option Pricing, SSE 50ETF Options, Hang Seng Index Options.

1 Introduction

As a cornerstone of modern financial markets, option pricing continues to pose significant challenges in accurate valuation, making it a persistent focus for both academics and practitioners. A major milestone in this area was the introduction of the Black-Scholes (BS) model in 1973 [1], which provided an analytical solution for pricing European-style options, and laid the theoretical foundation for modern derivatives pricing. Despite its influence, the BS model relies on several strong assumptions: 1) asset prices follow a log-normal distribution; 2) options are European, and can only be exercised at expiration; 3) short selling is allowed; 4) there are no transaction costs; 5) there are no dividends during the option's validity; 6) there are no arbitrage opportunities; and 7) trading is continuous. These assumptions are often violated in practice, resulting in significant discrepancies between theoretical valuations and actual market prices.

Moreover, the BS model is limited to European options, and does not generalize well to American or exotic derivatives.

To address these limitations, numerous alternative pricing models have been introduced, such as the jump diffusion model [2-5], stochastic volatility models [6-9], GARCH-type models [10-12], wavelet-based models [13-14], and deep learning approaches [15-17]. Among these, stochastic volatility models have gained widespread adoption for their ability in capturing empirical features of financial time series, including volatility clustering and time-varying dynamics.

The Heston model [18] is one of the most commonly adopted frameworks for modeling stochastic volatility. Its primary advantage lies in modeling volatility as a mean-reverting square root process, which aligns well with observed market behavior. Additionally, unlike many other stochastic volatility models, the Heston model offers a closed-form solutions for European option prices, improving computational tractability and facilitating practical implementation.

As a parametric model, the calibration of the Heston framework involves estimating a set of six key parameters:

$$\Omega = \{\theta, \kappa, V_t, \sigma, \rho, \lambda\},$$

where θ denotes the long-term price variance, κ represents the rate of mean reversion, V_t is the instantaneous variance, σ is the volatility of volatility, ρ is the correlation coefficient between two Brownian motions, and λ represents the market price of volatility risk. The calibration objective for the Heston model is typically formulated as a nonlinear least squares problem:

$$C_{min} = \arg\min_{\Omega} \sum_{i=1}^{n} \omega_i \{C_i^P(\Omega) - C_i^M\}^2, \tag{1}$$

where C_i^M and $C_i^{\mathrm{P}}(\Omega)$ are the market-observed and model-predicted option prices, respectively, ω_i is the sample weight, and n denotes the number of observed options.

Accurate parameter estimation is crucial for the Heston model's pricing performance. Existing estimation methods can generally be categorized into two categories: traditional algorithms [1, 19] and modern intelligent optimization algorithms [16, 20]. While traditional calibration methods often exhibit slow convergence, susceptibility to local optima, and challenges in conducting statistical inference, intelligent optimization techniques, particularly the Genetic Algorithm (GA) [21], have attracted widespread attention for their ability to perform global searches and handle complex optimization. Several studies have successfully applied GA to the calibration of the Heston model, reporting promising improvements in estimation accuracy and computational performance [22-24].

Nevertheless, premature convergence, where an algorithm quickly settles on a local rather than a global optimum, remains one of the most persistent challenges in conventional GA [23]. In response to this issue, [25] proposed the Multi-Population Genetic Algorithm (MPGA), which incorporates multiple independently evolving subpopulations initialized with distinct strategies. By periodically exchanging individuals across

subpopulations through an immigration operator [26], MPGA promotes population diversity, preserves elite individuals, and effectively mitigates premature convergence [27]. Since its introduction, MPGA has found extensive application across various optimization domains, such as lot sizing [27-28], flow shop scheduling [29-30], multi-label feature selection [31], binary classification [32], and predictive modeling [33].

Despite its demonstrated effectiveness in various domains, the application of MPGA to option pricing remains largely unexplored. To fill this gap, this study introduces a novel calibration framework for the Heston model (i.e, the MPGA-based estimation of the Heston option pricing model), which employs MPGA identify the optimal values of model parameters. The proposed approach is applied to calibrate and price options on both the SSE 50ETF and the Hang Seng Index. Empirical results show that MPGA not only effectively mitigates the premature convergence commonly observed in standard genetic algorithms but also significantly improves pricing accuracy.

The main contributions of this study are threefold: 1) it pioneers the use of MPGA for calibrating the Heston model, providing a robust and adaptable approach to option pricing; 2) the proposed framework is empirically validated in both developed and emerging markets, demonstrating its generalizability and practical relevance; and 3) an ask-bid weighting scheme is integrated into the calibration process to further improve pricing accuracy.

The remainder of the paper is organized as follows. Section 2 provides an overview of the Heston model. Section 3 details the calibration methodology based on MPGA. Section 4 presents the empirical analysis using option data from both the SSE 50ETF and the Hang Seng Index. Section 5 concludes the paper.

2 Heston Option Pricing Model

The Heston model [10] assumes the underlying stock price S_t follows a stochastic diffusion process:

$$dS_t = \mu S_t dt + \sqrt{V_t} S_t dW_t^1, \tag{2}$$

where μ is the drift term, V_t denotes the instantaneous variance of the stock price, and W_t^1 represents a Brownian motion. The variance V_t is modeled as a Cox-Ingersoll-Ross (CIR) process [34]:

$$\mathrm{d}V_t = \kappa(\theta - V_t)dt + \sigma\sqrt{V_t} dW_t^2, \tag{3}$$

where κ, θ, and σ are positive constants, W_t^2 is another Brownian motion. The correlation between the two Brownian motions (i.e., W_t^1 and W_t^2) is given by

$$dW_t^1 dW_t^2 = \rho dt, \tag{4}$$

where $\rho \in [-1,1]$ is a constant correlation coefficient.

Under the standard no-arbitrage principle, the price $U(S,V,t)$ of any derivative that depends on the stock price S and V satisfies the following partial differential equation (PDE) [1, 35]:

$$\frac{1}{2}VS^2\frac{\partial^2 U}{\partial S^2}+\rho\sigma VS\frac{\partial^2 U}{\partial S\partial V}+\frac{1}{2}\sigma^2V\frac{\partial^2 U}{V^2}+rS\frac{\partial U}{\partial S}+A_1\frac{\partial U}{\partial V}-rU+\frac{\partial U}{\partial t}=0, \quad (5)$$

where $A_1=\kappa[\theta-V]-\lambda(S,V,t)\sigma\sqrt{V}$, r is the risk-free interest rate, and $\lambda(S,V,t)$ represents the market price of volatility risk.

In the Heston model, the price $C(S,V,t)$ of a European call option satisfies the same PDE as Equation (5), with U replaced by C, i.e.,

$$\frac{1}{2}VS^2\frac{\partial^2 C}{\partial S^2}+\rho\sigma VS\frac{\partial^2 C}{\partial S\partial V}+\frac{1}{2}\sigma^2V\frac{\partial^2 C}{\partial V^2}+rS\frac{\partial C}{\partial S}+A_1\frac{\partial C}{\partial V}-rC+\frac{\partial C}{\partial t}=0. \quad (6)$$

Since $\lambda(S,V,t)$ is not directly observable, Heston assumes it is proportional to volatility:

$$\lambda(S,V,t)=\kappa\sqrt{V},$$

where κ is a constant.

Under the Heston model, the closed-form solution for pricing a European call option (assuming no dividends) is given by:

$$C(S,V,t)=SP_1-Ke^{-r(T-t)}P_2, \quad (7)$$

where K is the strike price, T is the maturity date, P_1 is the adjusted risk-neutral probability distribution functions, and P_2 is the risk-neutral probability distribution functions.

Due to the complexity of the pricing function, P_1 and P_2 are typically computed using the characteristic function approach combined with an inverse Fourier transform [36-37]:

$$P_j=\frac{1}{2}+\frac{1}{\pi}\int_0^{+\infty}Re\left[\frac{e^{-iuln(K)}f_j(S,V,T,u)}{iu}\right]du, \ \ j=1,2 \quad (8)$$

where i denotes the imaginary unit, $Re[\cdot]$ extracts the real component of a complex expression, and f_j represents the characteristic function of the log-asset price evaluated under the risk-neutral probability measure, i.e.,

$$f_j(S,V,T,u)=e^{-iu\ln(S)+C_j(T-t,u)+D_j(T-t,u)V}, \quad \tau=T-t. \quad (9)$$

The functions $C_j(\tau,u)$ and $D_j(\tau,u)$ are defined as:

$$C_j(\tau,u) = rui\tau + \frac{a}{\sigma^2}\left(b_j - \rho\sigma ui + d_j\right) - 2\ln\left(\frac{1-g_j e^{d_j\tau}}{1-g_j}\right),$$

$$D_j(\tau,u) = \frac{b_j-\rho\sigma ui+d_j}{\sigma^2}\left(\frac{1-e^{d_j\tau}}{1-g_j e^{d_j\tau}}\right),$$

where $d_j = \sqrt{\left(\rho\sigma ui - b_j\right)^2 + \sigma^2\left(2a_j ui - u^2\right)}$, $g_j = \frac{b_j-\rho\sigma ui+d_j}{b_j-\rho\sigma ui-d_j}$, $a = \kappa^*\theta^*$, $a_1 = \frac{1}{2}$, $a_2 = -\frac{1}{2}$, $b_1 = \kappa + \lambda - \rho\sigma$, and $b_2 = \kappa + \lambda$. Using the put-call parity, the price $P(\mathrm{S},\mathrm{V},\mathrm{t})$ of a European put option is then given by:

$$P(\mathrm{S},\mathrm{V},\mathrm{t}) = C(\mathrm{S},\mathrm{V},\mathrm{t}) + Ke^{-r(T-t)} - S. \tag{10}$$

Both the call and put option prices under the Heston model depend on six parameters, namely, $\Omega = \{\kappa,\theta,\sigma,\rho,V_t,\lambda\}$. Assuming $\lambda = 0$ under the risk-neutral measure, the number of parameters reduces to five, i.e., $\Omega = \{\kappa,\theta,\sigma,\rho,V_t\}$. Accordingly, this study focuses on the five-parameter Heston model for calibration and pricing.

3 MPGA-Based Estimation of the Heston Option Pricing Model

The genetic algorithm was proposed by Professor Holland in 1975 [38]. Over time, it has evolved into a class of adaptive search techniques widely studied in the literature [39-40], which essentially explore potential solutions through local modifications known as genetic operations, such as selection, crossover, and mutation. As a self-adaptive optimization algorithm, it iteratively improves solutions through recombination and reproduction, favoring individuals with higher fitness values [38]. To handle multiple tasks, [25] extended GA to MPGA by employing multiple subpopulations rather than a single population for genetic operations. Each subpopulation may utilize different selection, crossover, and mutation strategies, along with distinct crossover and mutation probabilities. Particularly, MPGA adopts a multi-population architecture, where subpopulations evolve independently and periodically exchange individuals. This structure enhances search diversity, speeds up convergence, and helps prevent entrapment in local optima by maintaining high-quality solutions across generations [26].

With the increasing prevalence of multi-core CPU architectures and parallel computing techniques, transitioning from GA to MPGA is straightforward. This study adopts a parallel population structure, where multiple subpopulations evolve independently using different genetic strategies. The migration operator transfers the best individuals from one subpopulation to others for further evolution. This process continues until the optimal solution is reached. Specifically, the implementation of MPGA mainly consists of initial population, encoding, fitness function, genetic operators, immigration operator, and iteration termination. Genetic operators includes selection, crossover, and mutation.

(1) Initial population

The initial population is the foundation of MPGA. This paper uses a completely randomized approach to generate multiple subpopulations. The number of subpopulations is chosen to balance computational memory constraints while ensuring a strong overall search capability.

(2) Encoding

Encoding plays a crucial role in genetic algorithms. Frequently adopted encoding strategies include binary, continuous, and symbolic forms. This study employs binary encoding for real-value representation of chromosomes. In the Heston option pricing model, each chromosome represents a parameter set to be estimated, and different chromosomes correspond to different parameter estimates. The advantage of binary encoding is its ability to efficiently track genetic algorithm evolution paths while maintaining simple encoding and decoding operations.

(3) Fitness function

The fitness function measures how well an individual chromosome (parameter set) performs in approximating the option price. It is derived from the objective function as follows:

$$f_k = \sum_{i=1}^{n} \omega_i [C_i^P(\Omega) - C_i^M]^2, \tag{11}$$

where C_i^P and C_i^M represent the model-predicted and market-observed option prices for the i-th sample, respectively, ω_i are weights, and f_k quantifies the pricing accuracy of the k-th individual in the population. The larger the value f_k, the worse the pricing effect and vice versa.

A proper choice of weights ω_i is crucial for optimization. Following [41], we use the ask-bid weighting scheme, where $\omega_i = \frac{1}{|ask_i - bid_i|}$, and the ask-bid spread $ask_i - bid_i$ represents pricing discrepancies between buyers and sellers, making it an effective weighting factor for option pricing analysis.

(4) Genetic Operators

GA employs three fundamental genetic operations: selection, crossover, and mutation. First, the selection process identifies individuals with superior fitness to propagate their genetic material. In this study, we adopt the random traversal sampling technique, which is recognized for its unbiased selection and low expansion of individual samples [23]. The selection probability p_k for an individual k is defined as

$$p_k = \frac{f_k}{\sum_{k=1}^{N} f_k},$$

where N is the population size. Higher fitness values result in a greater probability of selection.

Second, crossover operator is a process of facilitating recombination by exchanging genetic material between selected individuals. This study employs the single-point

crossover method, where a random crossover point is chosen in the gene string, and genetic material is swapped between two parents, generating two new offspring. For example,

$$\begin{aligned} &\text{Parent 1: } 10011|0101 \\ &\text{Parent 2: } 11001|0001 \end{aligned}$$

$$\Rightarrow \begin{aligned} &\text{Offsprings 1: } 10011|0001 \\ &\text{Offsprings 2: } 11001|0101 \end{aligned}$$

Third, mutation operator is a method of introducing diversity by randomly flipping gene values at selected positions with a given mutation probability p_m. For example, chromosome A = 11110001, mutating the third and fifth positions yields 11011001. Mutation helps refine local search performance, and prevents premature convergence.

In the genetic algorithm, crossover and mutation work in tandem, with the former promoting global exploration and the latter enhancing local search refinement. Their probabilities, p_c and p_m, play a critical role in balancing search strategies. Empirical values typically fall within the following ranges: crossover probability $p_c \in [0.7, 0.9]$ and mutation probability $p_m \in [0.001, 0.05]$.

(5) Immigration operator

The immigration operator allows for the exchange of high-fitness individuals among subpopulations, promoting diversity and preventing premature convergence. By spreading optimal solutions across populations, it enhances global search capability, accelerates convergence, and improves overall algorithm stability.

(6) Iteration Termination

Each repetition of steps (3) to (5) constitutes an iteration, with results from one iteration serving as the initial state for the next. MPGA employs two termination criteria: fixed iteration count, where the algorithm stops after a predefined number of generations, and fitness stability, where termination occurs if the optimal individual's fitness remains unchanged for several consecutive generations.

The MPGA flowchart (parallel population structure) is illustrated in Fig. 1.

4 Empirical Analysis: SSE 50ETF and Hang Seng Index Options

This study employs MPGA to estimate the parameters of the Heston model using Shanghai SSE 50ETF stock index options and Hong Kong Hang Seng Index options. The objective is to evaluate precision, accuracy, and effectiveness of MPGA in option pricing across a developing market (Mainland China) and a developed market (Hong Kong).

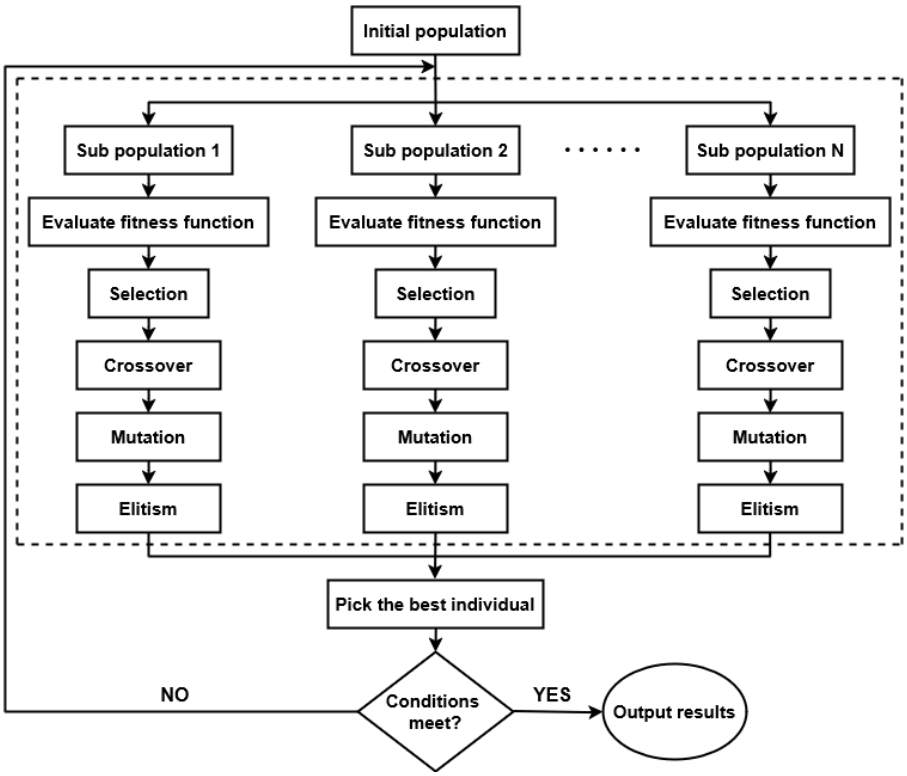

Fig. 1. MPGA flowchart (parallel population structure)

To ensure the validity of the data analysis, the following preprocessing steps are applied: 1) excluding options with zero trading volume; 2) removing options with remaining maturities exceeding 100 trading days; 3) filtering out call options that do not satisfy the arbitrage-free condition:

$$C_t \geq \max\left(S_t - \mathrm{K}e^{-r(T-t)}, 0\right),$$

where C_t and S_t are the option and stock price at time t, respectively, K is the strike price of the option, r is the risk-free interest rate, and T is the maturity date. According to the Put-Call Parity Theorem, every call option has a corresponding put option. Thus, this study focuses solely on call options.

Following the approach in [41], this paper introduces ask-bid weights into the proposed MPGA-based estimation framework for the Heston model. To evaluate the effectiveness of the ask-bid weighting scheme, an equal-weighting approach is also implemented for comparison. The performance of each scheme is assessed using three standard error metrics: mean squared error (MSE), root mean squared error (RMSE), and mean absolute error (MAE), defined respectively as:

$$MSE = \frac{1}{N}\sum_{i=1}^{N}(\hat{y}_i - y_i)^2,$$
$$RMSE = \sqrt{\frac{1}{N}\sum_{i=1}^{N}(\hat{y}_i - y_i)^2},$$
$$MAE = \frac{1}{N}\sum_{i=1}^{N}|\hat{y}_i - y_i|,$$

where $\hat{y}_i$ and y_i represent the model-predicted and market-observed option prices, respectively, and N is the number of observations. For all three metrics, the smaller the better.

In addition, to further assess the effectiveness of the proposed MPGA approach, we compare its performance with several benchmark methods, including random sequence Monte Carlo (MC), dual-variable Monte Carlo (Dual MC), control variable Monte Carlo (Control variable MC), Nonlinear Least Squares (NLS), and conventional GA. The Monte Carlo-based methods are implemented with 1,000 and 10,000 simulation iterations, respectively.

4.1 SSE 50ETF Stock Index Options

As the first derivative instrument in China's capital market, SSE 50ETF options hold significant pricing importance for option pricing research. This study utilizes a dataset of European call options on the SSE 50ETF with transaction data from March 11, 2019, to price the call options on May 7, 2019. The strike prices (in yuan) with expiration dates on March 27, April 24, and June 26, 2019 are 2.10, 2.15, 2.20, 2.25, 2.30, 2.35, 2.40, 2.45, 2.50, 2.55, 2.60, 2.65, 2.70, 2.75, 2.80, 2.85, 2.90, 2.95 and 3.00. The closing price of each option is taken as the average of the corresponding bid and ask prices. On March 27, 2019, the closing price of the SSE 50ETF was 2.69 yuan, and the 3-month SHIBOR was 0.0027565. When the time to expiration is less than 120 days, the 3-month SHIBOR is used as the risk-free rate [42-43]. All data are sourced from the Bloomberg database.

4.1.1 Parameter Estimation

For parameter estimation, we consider call options on March 11, 2019, and configure MPGA with 10 subpopulations of 40 individuals each, evolving over 200 generations. The crossover probability is randomly chosen within the range [0.7, 0.9], while the mutation probability is drawn from [0.001, 0.05]. Table 1 reports the resulting parameter estimates for the Heston model.

Table 1. Parameter estimates of the call option on March 11, 2019

κ	θ	σ	ρ	V_t
6.5992	0.0543	2.0130	-7.34E-05	0.1096

The final fitness value of the proposed algorithm is 5.37×10^{-6}, which is notably lower than those obtained by traditional NLS (5.54×10^{-6}) and GA (5.51×10^{-6}), indicating superior estimation accuracy. Fig. 2 illustrates the evolution of the average fitness values across subpopulations. Each generation is represented by ten dots, with each dot corresponding to the average fitness value of a distinct subpopulation.

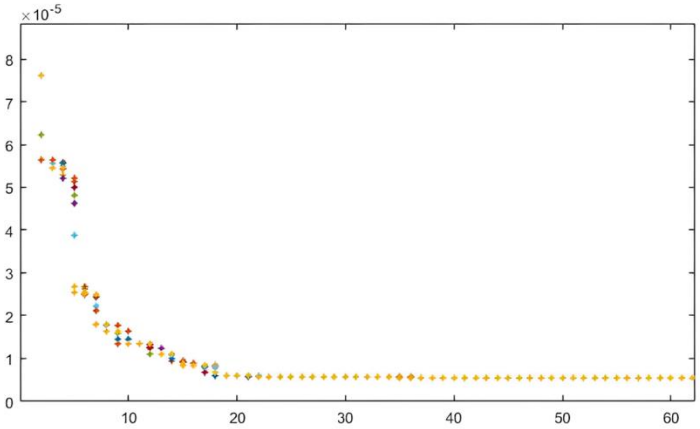

Fig. 2. Evolution of the average fitness of each sub-population for SSE 50ETF. Note: the x-axis denotes the number of generations, and the y-axis represents the fitness values.

During the first 20 generations, fitness values fluctuate substantially but gradually stabilize, confirming MPGA's effectiveness in optimizing Heston model parameters. Initially, the average fitness across all subpopulations is 8.38×10^{-6}, which steadily converges to 5.37×10^{-6} by generation 40, demonstrating MPGA's strong convergence properties. These results corroborate the findings reported in [23].

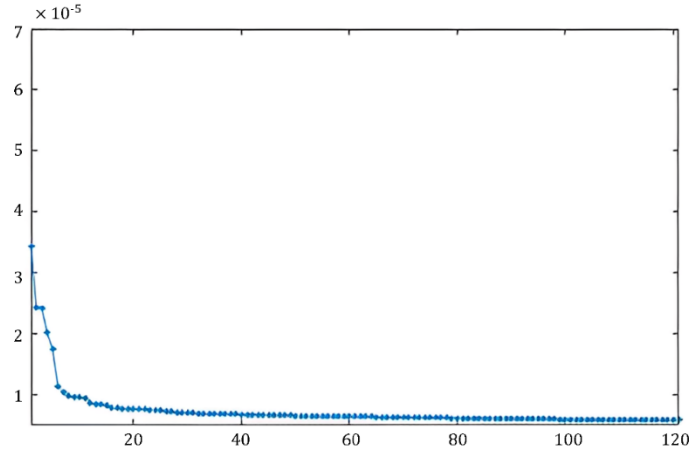

Fig. 3. Evolution of the best individual fitness value of each generation for 50ETF. Note: the x-axis denotes the number of generations, and the y-axis represents the fitness values.

Fig. 3 further depicts the best individual fitness value in each generation. After applying the immigration operator, the best fitness value exhibits an almost strictly decreasing trend, providing additional evidence of the effectiveness of the migration mechanism in MPGA.

4.1.2 Option Pricing Results

Using the estimated parameters, we price European call options with times to maturity of 0.0595, 0.1984, and 0.5595 years on May 7, 2019. The pricing results are reported in Table 2. On that date, the closing price of the SSE 50ETF was 2.79 yuan, and a 3-month SHIBOR was 0.0029220. The fourth and ninth columns of Table 2 list the actual closing prices of the options, while the fifth and tenth columns provide the predicted prices obtained using MPGA with ask-bid weights.

Table 2. Predicted prices via MPGA for SSE 50ETF on May 07, 2019.

No.	Maturity Date	Strike Prices	True Prices	Predicted Prices	No.	Maturity Date	Strike Prices	True Prices	Predicted Prices
1	0.0595	2.50	0.3071	0.3037	31	0.1984	2.95	0.0539	0.0729
2	0.0595	2.55	0.2562	0.2584	32	0.1984	3.00	0.0413	0.0605
3	0.0595	2.60	0.2099	0.2151	33	0.1984	3.10	0.0234	0.0422
4	0.0595	2.65	0.1558	0.1745	34	0.1984	3.20	0.0135	0.0300
5	0.0595	2.70	0.1160	0.1376	35	0.1984	3.30	0.0086	0.0218
6	0.0595	2.75	0.0824	0.1055	36	0.1984	3.40	0.0057	0.0161
7	0.0595	2.80	0.0534	0.0788	37	0.5595	2.20	0.6404	0.6497
8	0.0595	2.85	0.0368	0.0579	38	0.5595	2.25	0.6005	0.6052
9	0.0595	2.90	0.0246	0.0421	39	0.5595	2.30	0.549	0.5617
10	0.0595	2.95	0.0159	0.0305	40	0.5595	2.35	0.5046	0.5191
11	0.0595	3.00	0.0111	0.0221	41	0.5595	2.40	0.4612	0.4776
12	0.0595	3.10	0.0056	0.0117	42	0.5595	2.45	0.4195	0.4375
13	0.0595	3.20	0.0031	0.0062	43	0.5595	2.50	0.3793	0.3989
14	0.0595	3.30	0.0027	0.0034	44	0.5595	2.55	0.3421	0.3620
15	0.0595	3.40	0.0020	0.0018	45	0.5595	2.60	0.3109	0.3270
16	0.1984	2.20	0.6119	0.6108	46	0.5595	2.65	0.2769	0.2940
17	0.1984	2.25	0.5622	0.5633	47	0.5595	2.70	0.2462	0.2633
18	0.1984	2.30	0.5130	0.5163	48	0.5595	2.75	0.2204	0.2349
19	0.1984	2.35	0.4644	0.4700	49	0.5595	2.80	0.1924	0.2089
20	0.1984	2.40	0.4173	0.4245	50	0.5595	2.85	0.1674	0.1853
21	0.1984	2.45	0.3692	0.3801	51	0.5595	2.90	0.1466	0.1641
22	0.1984	2.50	0.3235	0.3370	52	0.5595	2.95	0.1286	0.1452
23	0.1984	2.55	0.2798	0.2956	53	0.5595	3.00	0.1118	0.1284

24	0.1984	2.60	0.2427	0.2563	54	0.5595	3.10	0.0834	0.1007
25	0.1984	2.65	0.2037	0.2195	55	0.5595	3.20	0.0620	0.0793
26	0.1984	2.70	0.1680	0.1858	56	0.5595	3.30	0.0453	0.0629
27	0.1984	2.75	0.1377	0.1556	57	0.5595	3.40	0.0335	0.0503
28	0.1984	2.80	0.1115	0.1293					
29	0.1984	2.85	0.087	0.1069					
30	0.1984	2.90	0.0679	0.0882					

Note: The unit for prices is Chinese Yuan, and the unit for time is year.

As shown in Table 2, the predicted prices closely align with the observed market prices. However, when the actual market price is low, the relative error, which is defined as the absolute price difference divided by the actual price, can appear disproportionately large. For example, in row 12, the actual market price is 0.00560, while the predicted price is 0.01129. Although the absolute difference is only 0.00569, the relative error reaches 101.6%. This phenomenon can be attributed to several factors. First, the small denominator amplifies the relative error. Second, while the Heston model presumes a fixed risk-free rate, real-world interest rates tend to fluctuate over time. Third, small residuals associated with low-price options have limited influence on the fitness function in Equation (11), and thus may be deprioritized during optimization.

In addition, prediction errors tend to increase as the expiration date approaches. This may be due to increased market activity and potential insider trading, which violate the assumptions of the Heston model. For options with the same expiration, both actual and predicted prices decrease as the strike price increases, and the prediction error tends to diminish accordingly. This pattern arises because a higher strike price lowers the intrinsic value of the option for the buyer, thereby reducing its market price.

Table 3 reports the MSE, MAE, and RMSE results for SSE 50ETF options under two weighting schemes: ask-bid weights and equal weights. The results clearly show that incorporating ask-bid weights leads to more accurate pricing outcomes compared to equal weighting, highlighting its effectiveness in improving model performance.

Table 3. Comparison results under two weighting schemes for SSE 50ETF.

	$\omega_i = 1/\lvert ask_i - bid_i \rvert$	$\omega_i = 1/n$
MSE	0.00024	0.00028
RMSE	0.01544	0.01573
MAE	0.01383	0.01433

Table 4 reports the comparison results under various calibration methods. As observed, the pricing accuracy of Monte Carlo-based approaches improves only marginally as the number of simulations increases from 1,000 to 10,000. In contrast, GA significantly outperforms the Monte Carlo methods, yielding notably lower errors across all three evaluation metrics. Moreover, the proposed MPGA consistently outperforms the standard GA, demonstrating superior optimization efficiency and pricing accuracy across all scenarios.

Table 4. Option price comparisons for SSE 50ETF

Methods	Number of simulation	MSE	MAE	RMSE
MC	10,000	0.00126	0.02824	0.03546
	1,000	0.00133	0.02839	0.03642
Dual MC	10,000	0.00119	0.02745	0.03456
	1,000	0.00124	0.02756	0.03526
Control variable MC	10,000	0.00118	0.02732	0.03438
	1,000	0.00119	0.02742	0.03454
NLS		0.01337	0.01337	0.04145
GA		0.00025	0.00504	0.01568
MPGA		0.00024	0.00477	0.01544

4.2 Hang Seng Index Options

In the Hang Seng Index Options analysis, we use the European call option from September 10, 2018, as the basis to price options on September 12, 2018. The dataset includes strike prices with maturities on September 27, October 30, and November 29, covering strike levels from 24,600 to 28,600 in increments of 200. On September 10, 2018, the closing price of the Hang Seng Index was 26,613.42. The Hong Kong Interbank Offered Rates (HIBOR) were 0.025556 on September 10 and 0.002554 on September 12, 2018. All data are sourced from the Bloomberg database. To ensure data reliability, options with zero transaction volume are excluded.

4.2.1 Parameter Estimation

The parameter settings follow that used for SSE 50ETF options. As shown earlier, the ask-bid weighting scheme improves pricing accuracy over equal weighting; therefore, we adopt the ask-bid weights in this analysis. The Heston model parameters estimated using this weighting method are

$$[\kappa, \theta, \sigma, \rho, V_t] = [27.6044, 0.0189, 1.3214, -0.3086, 0.0497].$$

The evolution of the average fitness value of each subpopulation during MPGA optimization is illustrated in Fig. 4. Each generation is represented by ten dots, with each dot corresponding to the average fitness value of a distinct subpopulation.

As shown in Fig. 4, the average fitness values within each subpopulation fluctuate markedly during the first 10 iterations. However, the fluctuations diminish with continued iterations, and the values ultimately converge toward zero. Overall, the fitness values exhibit a downward trend, confirming the convergence behavior of MPGA. This result is consistent with the findings for SSE 50ETF options.

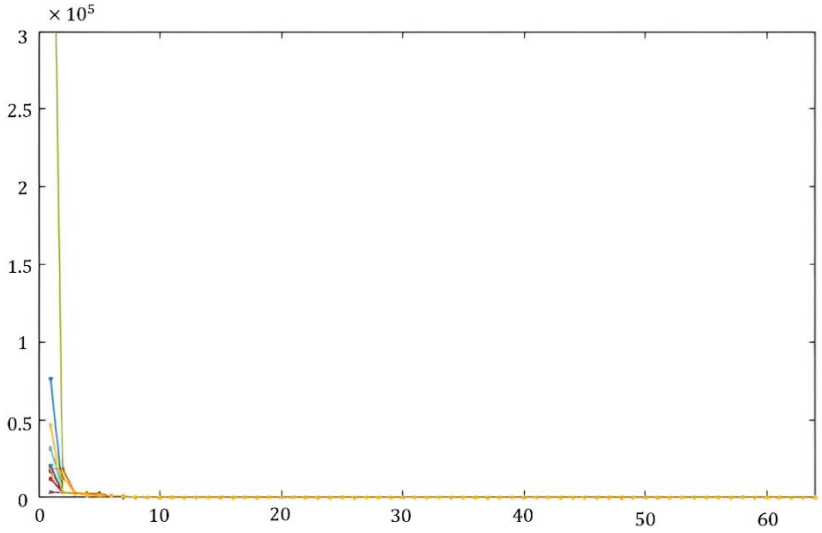

Fig. 4. Evolution of the average fitness of each sub-population for Hang Seng index options. Note: the x-axis denotes the number of generations, and the y-axis represents the fitness values.

4.2.2 Option Pricing Results

Using the calibrated parameters, we price call option on September 12, 2018. On that date, the closing price of the Hang Seng Index was 26,613.42, the 3-month HIBOR was 0.0025556, and the option maturities were $T = 0.0675$, $T = 0.1984$, and $T = 0.3175$ (in years). The pricing results are illustrated in Fig. 5.

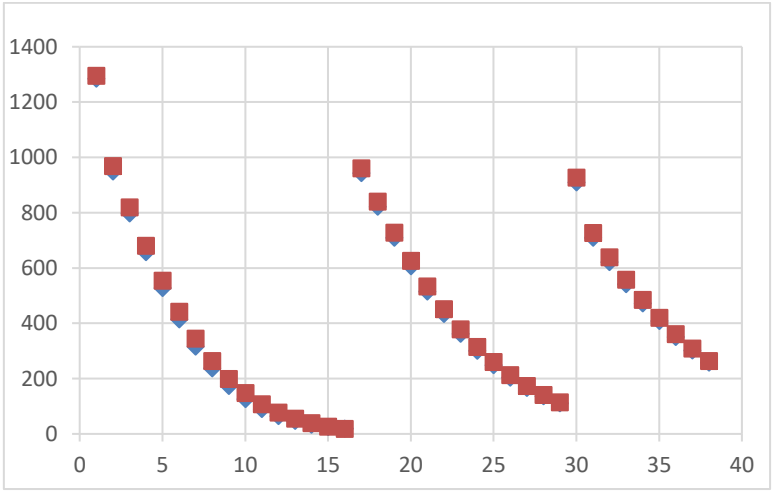

Fig. 5. Performance of MPGA for Hang Seng index options on September 12, 2018. Note: the blue ◆ denotes the true option price, and the orange ■ denotes the predicted values of the option price obtained by the calibrated parameters.

Consistent with prior findings, the option prices predicted by the MPGA-based Heston model closely match the actual market prices. As noted in [23], traditional genetic algorithms tend to exhibit larger prediction biases when market prices are relatively low. In contrast, MPGA effectively mitigates this issue by generating predicted prices that more closely align with observed transaction prices. For example, when the actual market price is 19, the MPGA-predicted price is 18, reflecting a notable improvement in accuracy. The close correspondence between predicted and actual prices further confirms the effectiveness and practical feasibility of MPGA-based calibration within the Heston framework, even in mature financial markets.

Table 5 presents the MSE, MAE, and RMSE results for Hang Seng index options under various calibration methods. The results indicate that the control variate Monte Carlo consistently outperforms both the standard Monte Carlo and dual-variable Monte Carlo in terms of pricing accuracy. Moreover, increasing the number of simulations leads to improved performance across all Monte Carlo-based approaches.

Table 5. Option price comparisons for Hang Seng index options.

Methods	Number of simulation	MSE	MAE	RMSE
MC	10,000	1443.297	31.609	37.991
	1,000	2211.029	37.939	47.022
Dual MC	10,000	1427.873	31.551	37.787
	1,000	2078.276	37.509	45.588
Control variable MC	10,000	1415.718	31.246	37.626
	1,000	1679.885	32.776	40.986
NLS		1045.791	25.215	32.339
GA		305.763	15.763	17.486
MPGA		282.060	8.493	16.795

Compared with GA and NLS, the proposed MPGA yields substantially more accurate price estimates. For instance, the MSEs of MPGA, GA, and NLS are 282.060, 305.763, and 1045.791, respectively, with the MSE of NLS being nearly four times higher than that of MPGA. Moreover, MPGA demonstrates a greater advantage over GA when market prices are higher. Specifically, for Hang Seng Index options, MPGA reduces the MSE by 8% compared to GA, whereas for SSE 50ETF options, the reduction is approximately 4%.

In summary, the results of both empirical analyses demonstrate that the proposed MPGA-based calibration framework substantially improves the predictive accuracy of the Heston model across both developing (Mainland China) and developed (Hong Kong) markets.

5 Conclusion

This study presents a novel approach to parameter estimation for the Heston option pricing model by employing a multi-population genetic algorithm to optimize model parameters. To evaluate the performance of the proposed approach, we conduct empirical analyses using option data from both a developing market (Mainland China, SSE 50ETF) and a developed market (Hong Kong, Hang Seng Index). The empirical results highlight several advantages of MPGA: 1) it consistently outperforms benchmark algorithms in identifying optimal parameter estimates; 2) it improves the accuracy of option pricing; and 3) it ensures a more stable and reliable evolutionary search process. Moreover, the option prices derived from MPGA calibration are closer to observed market prices, thereby yielding a more accurate implementation of the Heston model. Notably, the performance gain of MPGA is relatively modest when market prices are low, but becomes significantly more pronounced as prices increase.

For future research, two promising directions are identified. First, while optimization algorithms for European-style options are relatively mature, extending these methods to American-style options and other path-dependent derivatives remains a substantial challenge. Second, many pricing models adopted by exchanges are built on restrictive assumptions. Exploring techniques to relax these assumptions, and enhance model flexibility represents a valuable avenue for further investigation.

Acknowledgments. The authors would like to express their sincere gratitude to the editor and the three anonymous reviewers for their insightful comments and constructive suggestions. This research was supported by the National Social Science Foundation of China (Grant No. 21BTJ047).

Disclosure of Interests. The authors have no competing interests to declare.

References

1. Black, F., Scholes, M.: The pricing of options and corporate liabilities [J]. Journal of political economy, 81(3): 637-654 (1973)
2. Merton, R.C.: Option pricing when underlying stock returns are discontinuous [J]. Journal of financial economics, 3: 125-144 (1976)
3. Kou, S.G.: A jump-diffusion model for option pricing [J]. Management science, 48(8), pp.1086-1101 (2002)
4. Leippold, M., Vasiljević, N.: Pricing and disentanglement of American puts in the hyper-exponential jump-diffusion model [J]. Journal of Banking & Finance, 77: 78-94 (2017)
5. Ewald, C., Zou, Y.: Analytic formulas for futures and options for a linear quadratic jump diffusion model with seasonal stochastic volatility and convenience yield: Do fish jump? [J]. European Journal of Operational Research, 294(2), pp.801-815 (2021)
6. Scott, L.O.: Option pricing when the variance changes randomly: Theory, estimation, and an application [J]. Journal of Financial and Quantitative analysis, 22(4): 419-438 (1987)
7. Hull, J., White, A.: The pricing of options on assets with stochastic volatilities [J]. The journal of finance, 42(2): 281-300 (1987)

8. He, X.J., Lin, S.: A fractional Black-Scholes model with stochastic volatility and European option pricing [J]. Expert Systems with Applications, 178, p.114983 (2021)
9. He, X.J., Lin, S.: Analytically pricing foreign exchange options under a three-factor stochastic volatility and interest rate model: A full correlation structure [J]. Expert Systems with Applications, 246, p.123203 (2024)
10. Heston, S.L., Nandi, S.: A closed-form GARCH option valuation model [J]. The review of financial studies, 13(3): 585-625. (2000)
11. Li, B.: Option-implied filtering: evidence from the GARCH option pricing model [J]. Review of Quantitative Finance and Accounting, pp.1-21 (2019)
12. Escobar-Anel, M., Rastegari, J., Stentoft, L.: Option pricing with conditional GARCH models [J]. European Journal of Operational Research, 289(1), pp.350-363 (2021)
13. Haven, E., Liu, X. Shen, L.: De-noising option prices with the wavelet method. European Journal of Operational Research, 222(1), pp.104-112 (2012)
14. Liu, X., Cao, Y., Ma, C., Shen, L. Wavelet-based option pricing: An empirical study [J]. European Journal of Operational Research, 272(3), pp.1132-1142 (2019)
15. Andreou, P.C., Charalambous, C., Martzoukos, S.H.: Pricing and trading European options by combining artificial neural networks and parametric models with implied parameters [J]. European Journal of Operational Research, 185(3), pp.1415-1433 (2008)
16. Cao, Y., Liu, X., Zhai, J.: Option valuation under no-arbitrage constraints with neural networks [J]. European Journal of Operational Research, 293(1), pp.361-374 (2021)
17. Almeida, C., Fan, J., Freire, G., Tang, F.: Can a machine correct option pricing models?. Journal of Business & Economic Statistics, 41(3), pp.995-1009 (2023)
18. Heston, S.L.: A closed-form solution for options with stochastic volatility with applications to bond and currency options [J]. The review of financial studies, 6(2): 327-343 (1993)
19. Duffie, D., Pan, J., Singleton, K.: Transform analysis and asset pricing for affine jump-diffusions [J]. Econometrica, 68(6): 1343-1376 (2000)
20. Ivașcu, C.F.: Option pricing using machine learning [J]. Expert Systems with Applications, 163, p.113799 (2021)
21. Grace, B.K.: Black-Scholes option pricing via genetic algorithms [J]. Applied Economics Letters, 7(2): 129-132 (2000)
22. Mrázek, M., Pospíšil, J., Sobotka, T.: On calibration of stochastic and fractional stochastic volatility models. European Journal of Operational Research, 254(3), pp.1036-1046 (2016)
23. Li, B., and He, W.L.: New method of finding the parameters of Heston's Option Pricing Model. The Journal of Quantitative & Technical Economics, 3:129-145 (2015)
24. Yang, Z., Zhang, L., Tao, X., Ji, Y.: Heston-GA Hybrid Option Pricing Model Based on ResNet50. Discrete Dynamics in Nature and Society, 2022(1), p.7274598 (2022)
25. Kim, J., and Khosla, P.K.: A Multi-population Genetic Algorithm and Its Application to Design Of Manipulators. In Proceedings of the IEEE/RSJ International Conference on Intelligent Robots and Systems (Vol. 1, pp. 279-286). IEEE (1992)
26. Cochran, J.K., Horng, S.M., Fowler, J.W.: A multi-population genetic algorithm to solve multi-objective scheduling problems for parallel machines [J]. Computers & Operations Research, 30(7): 1087-1102 (2003)
27. Toledo, C.F.M., França, P.M., Morabito, R. Kimms, A.: Multi-population genetic algorithm to solve the synchronized and integrated two-level lot sizing and scheduling problem. International Journal of Production Research, 47(11), pp.3097-3119 (2009)
28. Toledo, C.F.M., De Oliveira, R.R.R., França, P.M.: A hybrid multi-population genetic algorithm applied to solve the multi-level capacitated lot sizing problem with backlogging. Computers & Operations Research, 40(4), pp.910-919 (2013)

29. Cui, H., Li, X., Gao, L.: An improved multi-population genetic algorithm with a greedy job insertion inter-factory neighborhood structure for distributed heterogeneous hybrid flow shop scheduling problem. Expert Systems with Applications, 222, p.119805 (2023)
30. Liu, F., Li, G., Lu, C., Yin, L., Zhou, J.: A tri-individual iterated greedy algorithm for the distributed hybrid flow shop with blocking. Expert Systems with Applications, 237, p.121667 (2024)
31. Park, J., Park, M.W., Kim, D.W., Lee, J.: Multi-population genetic algorithm for multilabel feature selection based on label complementary communication. Entropy, 22(8), p.876 (2020)
32. Zhang, W., He, H. Zhang, S.: A novel multi-stage hybrid model with enhanced multi-population niche genetic algorithm: An application in credit scoring. Expert Systems with Applications, 121, pp.221-232 (2019)
33. Cheng, F., Fan, T., Fan, D. Li, S.: The prediction of oil price turning points with log-periodic power law and multi-population genetic algorithm. Energy Economics, 72, pp.341-355 (2018)
34. Cox, J.C., Ingersoll, Jr. J.E., Ross, S.A.: An intertemporal general equilibrium model of asset prices [J]. Econometrica: Journal of the Econometric Society, 363-384 (1985)
35. Merton, R.C.: Theory of rational option pricing [J]. Theory of Valuation, 229-288.
36. Cox, J.C., Ross, S.A.: The valuation of options for alternative stochastic processes [J]. Journal of financial economics, 3(1-2): 145-166 (1976)
37. Gil-Pelaez, J.: Note on the inversion theorem [J]. Biometrika, 38(3-4): 481-482 (1951)
38. Holland, J.H.: Adaptation in natural and artificial systems: An introductory analysis with applications to biology, control and artificial intelligence. Ann Arbor: University of Michigan Press (1975)
39. Grefenstette, J.J., Gopal, R., Rosmaita, B.J., Gucht, D.V.: Genetic Algorithms for the Traveling Salesman Problem. In Proceedings of the 1st International Conference on Genetic Algorithms (pp. 160-168) (1985)
40. Mitchell, M.: An introduction to genetic algorithms. MIT press (1998)
41. Wang, L., Zhang, L., Liu, L.F.: Calibration of Heston's Option Pricing Model by Using Simulated Annealing Algorithm [J]. The Journal of Quantitative & Technical Economics, 28(9): 131-139 (2011)
42. Shu, J., Zhang, J.E.: Pricing S&P 500 index options under stochastic volatility with the indirect inference method [J]. Journal of Derivatives Accounting, 1(2): 171-186 (2004)
43. Christoffersen, P., Jacobs, K.: Which GARCH model for option valuation? [J]. Management science, 50(9): 1204-1221 (2004)